Mon. Not. R. Astron. Soc. **418,** 2715–2719 (2011) doi:10.1111/j.1365-2966.2011.19660.x

Vector dark energy and high-z massive clusters

Edoardo Carlesi,[1]★ Alexander Knebe,[1] Gustavo Yepes,[1] Stefan Gottlöber,[2] Jose Beltrán Jiménez[3,4] and Antonio L. Maroto[5]

[1]*Departamento de Física Teórica, Universidad Autónoma de Madrid, 28049 Cantoblanco, Madrid, Spain*
[2]*Leibniz Institut für Astrophysik, An der Sternwarte 16, 14482 Potsdam, Germany*
[3]*Institute de Physique Théorique and Center for Astroparticle Physics, Université de Genève, 24 quai E. Ansermet, 1211 Genève, Switzerland*
[4]*Institute of Theoretical Astrophysics, University of Oslo, 0315 Oslo, Norway*
[5]*Departamento de Física Teórica, Universidad Complutense de Madrid, 28040 Madrid, Spain*

Accepted 2011 August 18. Received 2011 July 7

ABSTRACT

The detection of extremely massive clusters at $z > 1$ such as SPT-CL J0546−5345, SPT-CL J2106−5844 and XMMU J2235.3−2557 has been considered by some authors as a challenge to the standard Λ cold dark matter cosmology. In fact, assuming Gaussian initial conditions, the theoretical expectation of detecting such objects is as low as $\leq$1 per cent. In this paper we discuss the probability of the existence of such objects in the light of the vector dark energy paradigm, showing by means of a series of N-body simulations that chances of detection are substantially enhanced in this non-standard framework.

Key words: methods: numerical – galaxies: haloes – cosmology: theory – dark matter.

1 INTRODUCTION

Present day cosmology is still failing to explain satisfactorily the nature of dark energy, which is supposed to dominate the energetic content of the Universe today and to be responsible for the current accelerated expansion. In the standard Λ cold dark matter (ΛCDM) model, this cosmic acceleration is generated by the presence of a cosmological constant. However, the required value for that constant turns out to be tiny when compared to the natural scale of gravity, namely the Planck scale. Thus, the gravitational interaction would hence be described by two-dimensional constants differing by many orders of magnitude, and this poses a problem of naturalness. This is the so-called 'cosmological constant problem' and it motivated to consider alternative explanations for the current acceleration of the universe by either modifying the gravitational interaction at large distances or introducing a new dynamical field.

Indeed, one of the main challenges of observational cosmology is exactly to devise new tests which could help discriminating between the constant or dynamic nature of dark energy. In this regard, several authors have recently pointed out that the observation of extremely massive clusters at high redshift, such as SPT-CL J2106−5844 (Foley et al. 2011; $z \simeq 1.18, M_{200} = (1.27 \pm 0.21) \times 10^{15}\,\mathrm{M}_{\odot}$), SPT-CL J0546−5346 (Brodwin et al. 2010; $z \simeq 1.07$, $M_{200} = (7.95 \pm 0.92) \times 10^{14}\,\mathrm{M}_{\odot}$) and XMMU J2235.3−2557 (Jee et al. 2009; $z \simeq 1.4$, $M_{200} = (7.3 \pm 1.3) \times 10^{14}\,\mathrm{M}_{\odot}$) may represent a major shortcoming of the ΛCDM paradigm, where the presence of such objects should be in principle strongly disfavoured (see e.g. Baldi & Pettorino 2011; Mortonson, Hu & Huterer 2011).

While, on the one hand, this tension could be solved keeping the standard scenario and relaxing the assumption of Gaussianity in the initial conditions (as proposed in Enqvist, Hotchkiss & Taanila 2011; Hoyle, Jimenez & Verde 2011), it could be as well possible to use this observations as a constraint for different cosmological models. In this work we look at the vector dark energy (VDE) model, where the role of the dark energy is played by a cosmic vector field (Beltrán Jiménez & Maroto 2008). By means of a series of N-body simulations, we study the large-scale clustering properties of this cosmology, computing the cumulative halo mass functions at different redshifts and comparing them to the predictions of the standard model. In this way, we are able to show that the VDE cosmology does indeed predict a higher abundance of massive haloes at all redshifts, thus enhancing the probability of observing such objects with respect to ΛCDM.

2 VECTOR DARK ENERGY

The action of the VDE model (see Beltrán Jiménez & Maroto 2008) can be written as

$$S = \int \mathrm{d}^4x\sqrt{-g}\left[-\frac{R}{16\pi G} - \frac{1}{4}F_{\mu\nu}F^{\mu\nu} - \frac{1}{2}\left(\nabla_\mu A^\mu\right)^2 + R_{\mu\nu}A^\mu A^\nu\right], \quad (1)$$

where $R_{\mu\nu}$ is the Ricci tensor, $R = g^{\mu\nu}R_{\mu\nu}$ the scalar curvature and $F_{\mu\nu} = \partial_\mu A_\nu - \partial_\nu A_\mu$. This action can be interpreted as the Maxwell term for a vector field supplemented with a gauge-fixing term and an effective mass provided by the Ricci tensor. It is interesting to note that the vector sector has no free parameters nor potential terms, being G the only dimensional constant of the theory.

★E-mail: edoardo.carlesi@uam.es

For a homogeneous and isotropic universe described by the flat Friedmann–Lemaître–Robertson–Walker metric :

$$ds^2 = dt^2 - a(t)^2\, \boldsymbol{dx}^2, \tag{2}$$

we have $A_\mu = (A_0(t), 0, 0, 0)$ so that the corresponding equations read

$$\ddot{A}_0 + 3H\dot{A}_0 - 3[2H^2 + \dot{H}]A_0 = 0, \tag{3}$$

$$H^2 = \frac{8\pi G}{3}\left[\rho_{\rm R} + \rho_{\rm M} + \rho_A\right], \tag{4}$$

with $H = \dot{a}/a$ the Hubble parameter and

$$\rho_A = \frac{3}{2}H^2A_0^2 + 3HA_0\dot{A}_0 - \frac{1}{2}\dot{A}_0^2, \tag{5}$$

the energy density associated to the vector field, while $\rho_{\rm M}$ and $\rho_{\rm R}$ are the matter and radiation densities, respectively. During the radiation and matter eras in which the dark energy contribution was negligible, we can solve equation (3) with $H = p/t$, where $p = 1/2$ for radiation and $p = 2/3$ for matter eras, respectively, that is equivalent to assume that $a \propto t^p$. In that case, the general solution is

$$A_0(t) = A_0^+ t^{\alpha_+} + A_0^- t^{\alpha_-}, \tag{6}$$

with $A_0^\pm$ constants of integration, $\alpha_\pm = -(1 \pm 1)/4$ in the radiation era and $\alpha_\pm = (-3 \pm \sqrt{33})/6$ in the matter era. After dark energy starts dominating, the equation of state abruptly falls towards $w_{\rm DE} \to -\infty$ as the Universe approaches $t_{\rm end}$, and the equation of state can cross the so-called phantom divide line (Nesseris & Perivolaropoulos 2007), so that we can have $w_{\rm DE}(z = 0) < -1$.

Using the growing mode solution in equation (6) we can obtain the evolution for the energy density as

$$\rho_A = \rho_{A_0}(1 + z)^\kappa, \tag{7}$$

with $\kappa = 4$ in the radiation era and $\kappa = (9-\sqrt{33})/2 \simeq -1.63$ in the matter era. Thus, the energy density of the vector field scales like radiation at early times so that the ratio $\rho_A/\rho_{\rm R}$ is constant during such a period. Moreover, the value of the vector field A_0 during that era is also constant hence making the cosmological evolution insensitive to the time at which we impose the initial conditions (as long as they are set well inside the radiation dominated epoch). Also, the required constant values of such quantities in order to fit observations are $\rho_A/\rho_{\rm R}|_{\rm early} \simeq 10^{-6}$ and $A_0^{\rm early} \simeq 10^{-4}M_{\rm p}$ which can arise naturally during the early universe, for instance, as quantum fluctuations. Furthermore, they do not need the introduction of any unnatural scale, thus, alleviating the naturalness or coincidence problem. On the other hand, when the Universe enters the era of matter domination, ρ_A starts growing relative to $\rho_{\rm M}$ eventually overcoming it at some point so that the dark energy vector field becomes the dominant component.

Once the present value of the Hubble parameter H_0 and the constant $A_0^{\rm early}$ during radiation (which fixes the total amount of matter $\Omega_{\rm M}$) are specified, the model is completely determined. In other words, this model contains the same number of parameters as ΛCDM, i.e. the minimum number of parameters of any cosmological model with dark energy. Notice, however, that in the VDE model the present value of the equation of state parameter $w_0 = -3.53$ is radically different from that of a cosmological constant [cf. Fig. 1, where the redshift evolution of $\omega(z)$ is shown the range of our simulations]. Despite this fact, VDE is able to simultaneously fit supernovae (SNe) and cosmic microwave background (CMB) data with comparable goodness to ΛCDM (Beltrán Jiménez & Maroto 2008; Beltrán Jiménez, Lazkoz & Maroto 2009).

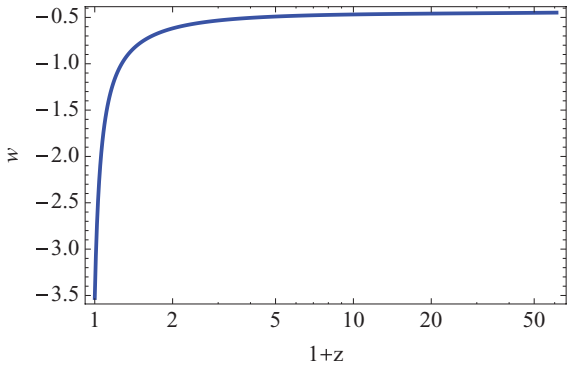

Figure 1. Equation of state of the VDE model for the best fit to SNIa data, shown in the range of our simulations.

3 THE DATA

3.1 Simulations

We wanted to estimate the probability of finding massive clusters at $z > 1$ in the VDE scenario compared to the ΛCDM one by means of CDM only N-body simulations. For this purpose, we chose to use a suitably modified version of the publicly available GADGET-2 code (Springel 2005), which had to take into account the different expansion history that characterizes the two cosmologies. In Table 1 we show the cosmological parameters used in the different simulations. For the VDE model, we have used the value of $\Omega_{\rm M}$ provided by the best fit to Type Ia SN (SNIa) data; the remaining cosmological parameters have been obtained by a fit to the *Wilkinson Microwave Anisotropy Probe* 7-year (*WMAP*7) CMB data of the model. w_0 denotes the present value of the equation of state parameter of dark energy. For ΛCDM we used the MultiDark simulation (Prada et al. 2011) cosmological parameters with a *WMAP*7 σ_8 normalization (Larson et al. 2011). In addition, we also simulated a ΛCDM-vde model, which implements the VDE values for $\Omega_{\rm M}$ and σ_8 in an otherwise standard ΛCDM picture. Although this model is certainly ruled out by current cosmological constraints, it provides none the less an interesting case study that allows us to disentangle the effects of these two cosmological parameters on structure formation in the VDE model.

We chose to run a total of eight 512^3 particles simulations summarized in Table 2 and explained below:

(i) a VDE (and a ΛCDM started with the same seed for the phases of the initial conditions) simulation in a $500\,h^{-1}$ Mpc box;

(ii) a second VDE (and again corresponding ΛCDM) simulation in a $1\,h^{-1}$ Gpc box;

(iii) two more VDE simulations with a different random seed, one in a $500\,h^{-1}$ Mpc and one in a $1\,h^{-1}$ Gpc box, as a check for the influence of cosmic variance;

(iv) two ΛCDM-vde simulations in a 500 and a $1000\,h^{-1}$ Mpc box.

Table 1. Cosmological parameters for ΛCDM, ΛCDM-vde and VDE.

Model	$\Omega_{\rm m}$	$\Omega_{\rm de}$	w_0	σ_8	h
ΛCDM	0.27	0.73	−1	0.8	0.7
ΛCDM-vde	0.388	0.612	−1	0.83	0.7
VDE	0.388	0.612	−3.53	0.83	0.62

Table 2. *N*-body settings used for the GADGET-2 simulations, the two $500\,h^{-1}$ Mpc and the two $1\,h^{-1}$ Gpc have the same initial random seed and starting redshift $z_{\rm start} = 60$ in order to allow for a direct comparison of the halo properties. The number of particles in each was fixed at 512^3. The box size B is given in h^{-1} Mpc and the particle mass in $h^{-1}\,{\rm M}_\odot$.

Simulation	B	$m_{\rm p}$
2 VDE-0.5	500	1.00×10^{11}
2 VDE-1	1000	8.02×10^{11}
ΛCDM-0.5	500	6.95×10^{10}
ΛCDM-1	1000	5.55×10^{11}
ΛCDM-0.5vde	500	1.00×10^{11}
ΛCDM-1vde	1000	8.02×10^{11}

The full set of simulations will be presented and analysed in more detail in an upcoming companion paper; in this paper, instead, we chose to focus on some of them only in order to gather information on large-scale structures and massive cluster at high redshift, respectively, in the two cosmologies. To this extent, the use of the same initial seed for generating the initial conditions in the coupled ΛCDM versus VDE simulations allows us to directly compare the structures identified by the halo finder.

As a final remark, we underline here that the choice of the boxes was made in order to allow the study of clustering on larger scales, without particular emphasis on low-mass objects, e.g. dark matter haloes with $M < 10^{14}\,h^{-1}\,{\rm M}_\odot$. This means that even though our halo finder has been able to identify objects down to $\sim 10^{12}\,h^{-1}\,{\rm M}_\odot$ in the $500\,h^{-1}$ Mpc box and $\sim 10^{13}\,h^{-1}\,{\rm M}_\odot$ in the $1\,h^{-1}$ Gpc one (which corresponds to a lower limit of 20 particles, see below), we are not comparing the mass spectrum at this far end. Therefore, since we are only interested in studying the behaviour of the mass function of these models at the very high mass end, in the following sections we will mostly refer to the ΛCDM-1, ΛCDM-vde and VDE-1 simulations, where we have a larger statistics for the supercluster scales.

3.2 Halo finding

In order to identify haloes in our simulation we have run the MPI+OpenMP hybrid halo finder AHF described in detail in Knollmann & Knebe (2009). AHF is an improvement of the MHF halo finder (Gill, Knebe & Gibson 2004), which locates local overdensities in an adaptively smoothed density field as prospective halo centres. The local potential minima are computed for each of these density peaks and the gravitationally bound particles are determined. Only peaks with at least 20 bound particles are considered as haloes and retained for further analysis, even though here we focus on the most massive objects only.

The mass of each halo is then computed via the equation $M(r) = \Delta\rho_{\rm c} 4\pi r^3/3$, where we applied $\Delta = 200$ as the overdensity threshold. Using this relation, particular care has to be taken when considering the definition of the critical density $\rho_{\rm c} = 3H^2/8\pi G$ because it involves the Hubble parameter, that differs substantially at all redshifts in the two models. This means that, identifying the halo masses, we have to take into account the fact that the value of $\rho_{\rm c}$ changes from ΛCDM to VDE. This has been incorporated into and taken care of in the latest version of AHF where $H_{\rm VDE}(z)$ is being read in from a pre-computed table.

We would like to mention that we checked that the objects obtained by this (virial) definition are in fact in equilibrium. To this extent we studied the ratio between two times kinetic over potential energy $2T/|U|$ confirming that at each redshift under investigation here this relation is equally well fulfilled for the ΛCDM and – more importantly – the VDE simulations (not presented here though). We therefore conclude that our adopted method to define halo mass in the VDE model leads to unbiased results and yields objects in equilibrium – as is the case for the ΛCDM haloes.

4 THE RESULTS

4.1 Mass function

With the halo catalogues at our disposal, we computed the cumulative mass functions $n(>M)$ at various redshifts. We show in Fig. 2 the results for the $1\,h^{-1}$ Gpc simulations at redshifts $z = 1.4$, 1.2, 1.1 and 0. This plot is accompanied by Table 3 where we list the masses of the most massive haloes found in each model and the redshifts under consideration.

We notice that the mass function for objects with $M > 10^{14}\,h^{-1}\,{\rm M}_\odot$ is several times larger in VDE than in ΛCDM at all redshifts, i.e. the number of high-mass haloes in this non-standard cosmological model is significantly increased. In particular, at this mass scale the VDE mass function is about three times larger at the relevant redshifts $z = 1.4, 1.2$ and 1.1 – and even larger at today's time.

In order to verify that this feature of the VDE model is not a simple reflection of cosmic variance (which should affect in particular the high-mass end, where the statistics is small) we compared the results presented in Fig. 2 to the mass functions of the set of two additional simulations started from a different random seed for the initial conditions confirming aforementioned results.

An interesting remark we would like to add here is that the physical mass (obtained dividing by the corresponding h values the values quoted in $h^{-1}\,{\rm M}_\odot$ units) of the largest haloes in the VDE-1 simulation at $z = 1.4$, 1.2 and 1.1 are perfectly compatible with the ones of the above clusters referred to in the Introduction, whereas the corresponding ΛCDM candidates are outside the 2σ compatibility level. And again, similar massive clusters have also been found in the duplicate VDE-1 simulation with a different initial seed.

Comparing the ΛCDM-1vde to the VDE-1 simulation at different redshifts, we note that while the two mass functions are almost indistinguishable for $M < 10^{14}\,h^{-1}\,{\rm M}_\odot$, on the higher mass end the former even outnumbers the latter by approximately ∼3. In the hierarchical picture of structure formation, we can attribute this relative difference to dynamical effects caused by the different expansion histories [based upon different $H(z)$] at later times $z \approx 1$, when the most massive structures actually start to form. In general, however, the ΛCDM-vde analysis shows that the enhancement seen in the VDE mass function with respect to ΛCDM is clearly driven by the higher values of $\Omega_{\rm M}$ and σ_8, a result expected since the abundance of clusters sensitively depends on the product of these two parameters (cf. Huterer & White 2002). On the one hand, this complicates the issue of model selection, since (although disfavoured by the *WMAP*7 data) we could invoke a (slightly) larger $\Omega_{\rm M}$ or a higher σ_8 normalization at $z = 0$ for ΛCDM trying to alleviate the current tension with the high-z massive clusters observations. On the other hand, the distinct expansion history that characterizes and differentiates between the two ΛCDM and VDE models would still leave a

Table 3. The most massive halo found in the three $1\,h^{-1}$ Gpc simulations (in units of $10^{14}\,h^{-1}\,\mathrm{M}_{\odot}$) as a function of redshift.

z	ΛCDM-1	VDE-1	ΛCDM-1vde
1.4	4.16	5.63	6.47
1.2	5.13	6.51	8.16
1.1	6.01	7.63	10.2
0	18.1	31.6	35.1

clear imprint on structure formation, which could be detected by, for instance, measuring σ_8's dependence on redshift. Such a test would indeed provide invaluable information for the study of ΛCDM and for any cosmological model beyond it such as VDE.

4.2 Probability

In order to provide a more quantitative estimate of the relative probability of observationally detecting such massive clusters at the indicated redshifts we used $n(>M, z)$ – the expected cumulative number density of objects above a threshold mass M as a function of redshift as given by our simulations – and integrated it over the comoving volume V_c of the survey:

$$N(>M) = \int_{\Delta z, \Omega_{\mathrm{survey}}} n(>M, z)\, \mathrm{d}V_c(z), \tag{8}$$

where Δz and Ω_{survey} are the redshift interval and the fraction of the sky covered by the survey to which we want to compare our theoretical expectations.

While $n(>M, z)$ can be readily calculated in ΛCDM cosmologies (e.g. Press & Schechter 1974; Sheth & Tormen 1999; Jenkins et al. 2001; Tinker et al. 2008), in VDE we have to devise a strategy to compute it based upon our numerical results only. We chose to adjust the formula of Sheth & Tormen (1999) as follows:

(i) we calculated the cumulative number densities in the desired redshift intervals Δz based upon our simulation data;

(ii) we adjusted the parameters of the Sheth–Tormen mass function fitting the numerical cumulative number densities derived from the VDE-1 and VDE-0.5 simulations;

(iii) we used these best-fitting estimates to analytically compute $n(>M, z)$ now having access to masses even outside our numerically limited range to be used with equation (8).

The results of the numerical integration over the comoving volumes (obtained using the limits quoted in the observational papers by Jee et al. 2009; Brodwin et al. 2010; Foley et al. 2011) are listed in Table 4 for the VDE, ΛCDM-vde and ΛCDM model. We can clearly see that the chances are substantially larger in the VDE model to find such massive objects than in ΛCDM; the numbers for VDE is in fact comparable to our fiducial ΛCDM-vde model confirming their relation to the enhanced values of Ω_{M} and σ_8. However, note that while the VDE model is compliant with both SNIa and CMB data the ΛCDM-vde is obviously ruled out

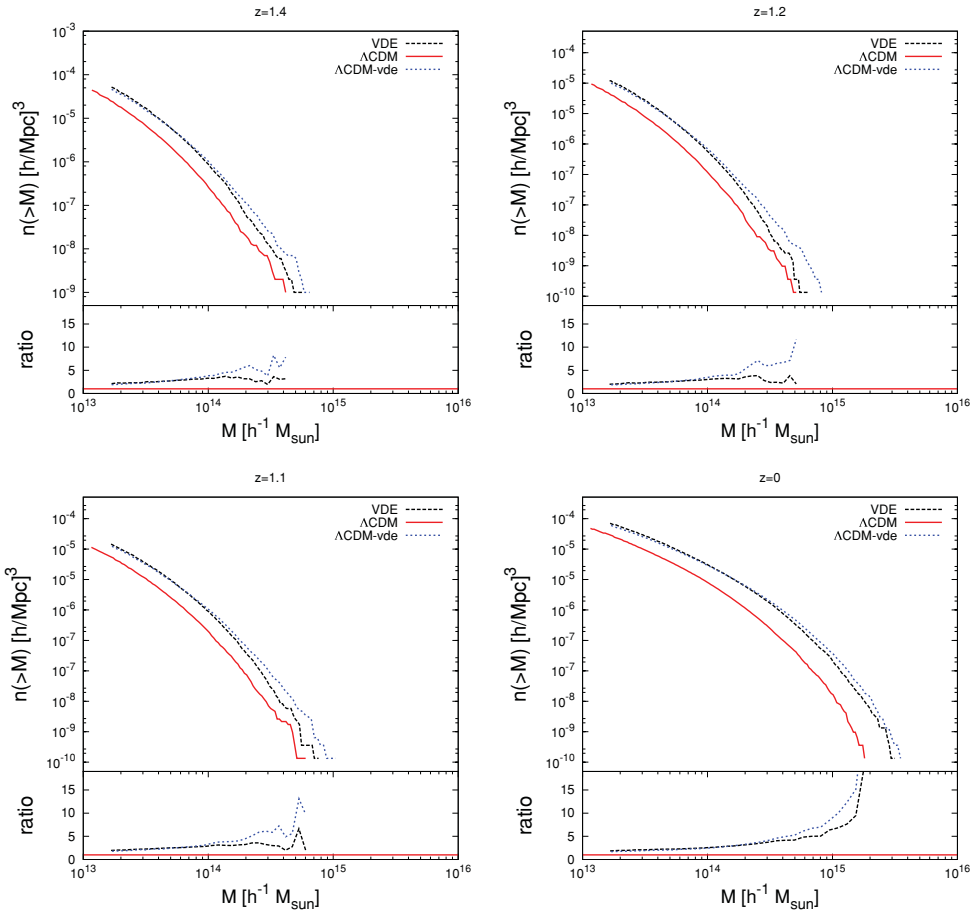

Figure 2. Mass functions (and their ratios) as computed for the VDE-1, ΛCDM-1 and ΛCDM-1vde simulations at $z = 1.4, 1.2, 1.1$ and 0. These redshifts have been chosen in order to overlap with the aforementioned observed massive clusters.

Table 4. Expected number of objects $N(>M)$ in excess of mass M and inside a certain (comoving) volume in the ΛCDM and VDE for different mass thresholds and survey volumes. Solid angles Ω are measured in deg^2 and masses are measured in $10^{14}\,h^{-1}\,\mathrm{M}_\odot$.

M	Δz	$\Omega_{\rm survey}$	$N_{\Lambda\rm CDM}$	$N_{\rm VDE}$	$N_{\Lambda\rm CDM-vde}$
>10	>1	2500	0.007	0.02	0.04
>7	>1	2500	0.03	0.31	0.56
>5	1.38–2.2	11	0.005	0.06	0.07

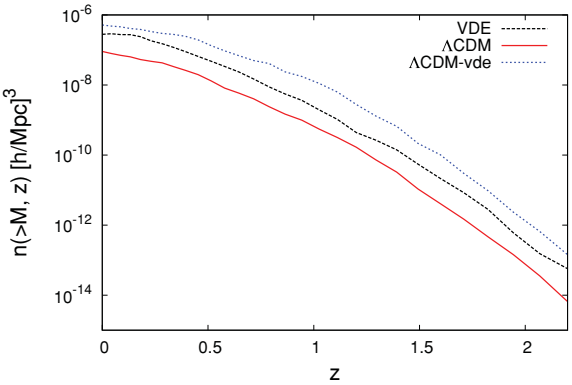

Figure 3. Numerical cumulative number densities of objects with $M > 5 \times 10^{14}\,h^{-1}\,\mathrm{M}_\odot$ for VDE, ΛCDM and ΛCDM-vde.

observationally. We complement these results with Fig. 3 where we plot the abundance evolution of clusters with mass $M > 5 \times 10^{14}\,h^{-1}\,\mathrm{M}_\odot$ computed utilizing above described procedure again. This plot confirms our previous analysis of the mass functions and shows that the expectation of massive objects is amplified in VDE by a factor of ∼3 to ∼10 over the considered redshift range, a factor which is even higher for the discretionary ΛCDM-vde. We would like to remark here that while our ΛCDM estimate for XMMU J2235.3−2557 is in agreement with the result quoted by Jee et al. (2009) (obtained using the same approach as here), the calculation done for SPT-CL J2106−5844 leads to an estimate substantially smaller than the one quoted by Foley et al. (2011), calculated using a Monte Carlo technique. However, this does not affect our conclusions, which are based on the comparison of results obtained in a consistent manner for the two models.

5 CONCLUSIONS

The observation of massive clusters at $z > 1$ provides an additional, useful test for the ΛCDM and other cosmological models beyond the standard paradigm. In this paper we have shown that the VDE scenario (Beltrán Jiménez & Maroto 2008) might account for such observations better than the ΛCDM concordance model, since the relative abundance of extremely massive clusters with $M > 5 \times 10^{14}\,h^{-1}\,\mathrm{M}_\odot$ is at all redshifts higher in this non-standard cosmology: the expected number of massive clusters is enhanced in VDE by at least a factor of ∼3 to find an object such as SPT-CL J2106−5844 at redshift $z \approx 1.2$ (Foley et al. 2011) and a factor of ∼10 for the other two observed clusters SPT-CL J0546−5346 (Brodwin et al. 2010) and XMMU J2235.3−2557 (Jee et al. 2009). Of course, these results might as well simply point in the direction of modifying the standard paradigm, for example including non-Gaussianities in the initial conditions or either using a higher σ_8 or $\Omega_{\rm M}$ value for the ΛCDM as the comparison to the ΛCDM-vde model seems to suggest.

None the less, this first results on the large-scale clustering in the case of VDE cosmology point in the right direction, significantly enhancing the probability of producing extremely massive clusters at high redshift as recent observations seem to require. For a more elaborate discussion and comparison of the VDE to the ΛCDM model (not solely focusing on massive clusters) we though refer the reader to the companion paper (Carlesi et al., in preparation).

ACKNOWLEDGMENTS

EC is supported by the MareNostrum project funded by the Spanish Ministerio de Ciencia e Innovacion (MICINN) under grant no. AYA2009-13875-C03-02 and MultiDark Consolider project under grant CSD2009-00064. AK acknowledges support by the MICINN's Ramon y Cajal programme as well as the grants AYA 2009-13875-C03-02, AYA2009-12792-C03-03, CSD2009-00064, and CAM S2009/ESP-1496. GY acknowledges support from MICINN's grants AYA2009-13875-C03-02 and FPA2009-08958. JBJ is supported by the Ministerio de Educación under the post-doctoral contract EX2009-0305 and also wishes to acknowledge support from the Norwegian Research Council under the YGGDRASIL programme 2009-2010 and the NILS mobility project grant UCM-EEA-ABEL-03-2010. We also acknowledge support from MICINN (Spain) project numbers FIS 2008-01323, FPA 2008-00592 and CAM/UCM 910309.

REFERENCES

Baldi M., Pettorino V., 2011, MNRAS, 412, L1
Beltrán Jiménez J., Maroto A. L., 2008, Phys. Rev. D, 78, 063005
Beltrán Jiménez J., Lazkoz R., Maroto A. L., 2009, Phys. Rev. D, 80, 023004
Brodwin M. et al., 2010, ApJ, 721, 90
Enqvist K., Hotchkiss S., Taanila O., 2011, J. Cosmol. Astropart. Phys., 4, 17
Foley R. et al., 2011, ApJ, 731, 86
Gill S. P. D., Knebe A., Gibson B. K., 2004, MNRAS, 351, 399
Hoyle B., Jimenez R., Verde L., 2011, Phys. Rev. D, 83, 103502
Huterer D., White M., 2002, ApJ, 578, L95
Jee M. et al., 2009, ApJ, 704, 672
Jenkins A., Frenk C. S., White S. D. M., Colberg J. M., Cole S., Evrard A. E., Couchman H. M. P., Yoshida N., 2001, MNRAS, 321, 372
Knollmann S. R., Knebe A., 2009, ApJS, 182, 608
Larson D. et al., 2011, ApJS, 192, 16
Mortonson M. J., Hu W., Huterer D., 2011, Phys. Rev. D, 83, 023015
Nesseris S., Perivolaropoulos L., 2007, J. Cosmol. Astropart. Phys., 0701, 018
Prada F., Klypin A. A., Cuesta A. J., Betancort-Rijo J. E., Primack J., 2011, arXiv e-prints
Press W. H., Schechter P., 1974, ApJ, 187, 425
Sheth R. K., Tormen G., 1999, MNRAS, 308, 119
Springel V., 2005, MNRAS, 364, 1105
Tinker J., Kravtsov A. V., Klypin A., Abazajian K., Warren M., Yepes G., Gottlöber S., Holz D. E., 2008, ApJ, 688, 709

This paper has been typeset from a TEX/LATEX file prepared by the author.